Tunable electric and magnetic properties of $Co_xZn_{1-x}S$ nanowires

Ming-Yen Lu,[1] Lih-Juann Chen,[1,a)] Wenjie Mai,[2] and Zhong Lin Wang[2,b)]
[1]*Department of Materials Science and Engineering, National Tsing Hua University, Hsinchu, Taiwan 30043, Republic of China*
[2]*School of Materials Science and Engineering, Georgia Institute of Technology, Atlanta, Georgia 30332-0245, USA*

(Received 13 October 2008; accepted 28 November 2008; published online 16 December 2008)

We report the growth of ZnS nanowires doped with cobalt using a one-step thermal evaporation method. The magnetism of the nanowires was maintained at room temperature, and the saturated magnetization increased with cobalt contents. Current-voltage measurements of a single nanowire showed not only a linear relationship, which implies Ohmic contacts of nanowire devices, but also tunable conductivities by doping concentration. © *2008 American Institute of Physics*.
[DOI: 10.1063/1.3050537]

Zinc sulfide (ZnS) is an important II-IV semiconducting material with a wide bandgap energy of 3.7 eV and a large exciton binding energy (~40 meV). Its nanostructures have been studied extensively in recent years. In addition to nanowires,[1,2] nanobelts,[3] and nanoparticles,[4] some fascinating morphologies have also been reported.[5–7] Due to its excellent properties of luminescence and photochemistry, ZnS have versatile potential applications as optoelectronic devices, e.g., ultraviolet light-emitting diodes and injection lasers,[8] infrared windows,[9] and flat-panel displays.[10]

On the other hand, the intrinsic properties of semiconductor, e.g., electrical,[11] luminescent,[12] and magnetic[13] properties, can be permanently modified by introducing impurities as dopants. Owing to the partially filled *d* or *f* valence electron states of transition metals, semiconductors doped with transition metals may possess magnetic properties. Partially filled *d* or *f* valence electron states contain unpaired electrons, in accordance with their spin, that may exhibit a magnetic phenomenon. This kind of semiconductors are called dilute magnetic semiconductors (DMSs).[14] Great efforts have been devoted to the research of DMS recently because of their potential applications in spintronic devices, such as spin-valve transistors, spin light-emitting diodes, and nonvolatile memory.[15,16]

In this regard, one-dimensional DMS materials at the nanometer scale, i.e., nanowires and nanoribbons, are expected to have interesting magnetoelectronic properties and could be a good candidate for realizing spintronic devices. Herein we report single-crystalline DMS $Co_xZn_{1-x}S$ nanowires with different doping levels. The nanowires were grown via the vapor-liquid-solid (VLS) mechanism with Au droplet on the top of nanowires. Superconducting quantum interference device (SQUID) measurements show that $Co_xZn_{1-x}S$ nanowires still maintain magnetism at room temperature. Furthermore, the electron transport properties of $Co_xZn_{1-x}S$ nanowires show the dependence of different doping concentrations.

The growth of $Co_xZn_{1-x}S$ nanowires was carried out by thermal evaporation under controlled conditions. An alumina tube was mounted horizontally inside a tube furnace. 0.2, 0.4, and 0.6 g of $CoCl_2 \cdot 6H_2O$ powders as the dopants source were located upstream (700 °C). The main source of 0.5 g ZnS powders was placed at the center of the furnace. The 4 nm Au/Al_2O_3 (11-20) substrates were downstream (700 °C). After the tube had been sealed and evacuated to a pressure of 1×10^{-1} torr, a carrier gas of 50 SCCM (SCCM denotes cubic centimeter per minute at STP) Ar+5% H_2 was kept flowing through the tube. During the growth, the pressure inside the tube was kept at 0.6 torr. The ZnS source powder was heated at a rate of 20 °C/min to 800 °C and kept for 30 min. After growth, the samples were cooled to room temperature in the furnace.

The morphology of the as-prepared ZnS nanowires with about 5.16% Co content was analyzed using field-emission scanning electron microscopy (SEM) (JEOL JSM-6500F), which is shown in Fig. 1(a). A high density of nanowires has a uniform diameter in the range of 50–100 nm and length up

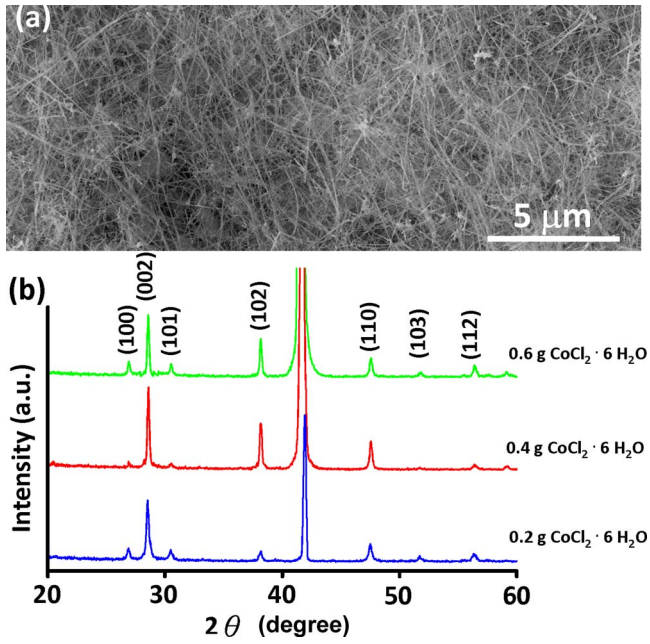

FIG. 1. (Color online) (a) A typical SEM image of $Co_xZn_{1-x}S$ nanowires with 0.6 g $CoCl_2 \cdot 6H_2O$. (b) XRD spectrum of $Co_xZn_{1-x}S$ nanowires with different amounts of $CoCl_2 \cdot 6H_2O$ doping source indicating the absence of the second phase in each sample.

a)Electronic mail: ljchen@mx.nthu.edu.tw.
b)Electronic mail: zhong.wang@mse.gatech.edu.

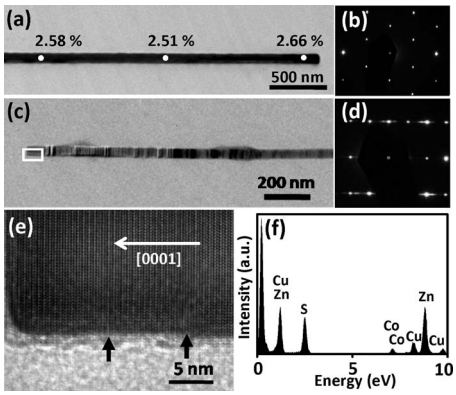

FIG. 2. (a) TEM image and (b) diffraction pattern of the $Co_xZn_{1-x}S$ nanowire with 2.59% Co content. Localized cobalt at. % of different parts of an individual $Co_xZn_{1-x}S$ nanowire are also shown in (a), demonstrating that cobalt ions are uniformly distributed in nanowires. (c) TEM image and (d) diffraction pattern of nanowire with 5.16% Co content. The corresponding atomic resolution image is shown in (e). Black arrows indicate the planar defects in the nanowire. (f) shows an EDS spectrum of $Co_xZn_{1-x}S$ nanowires.

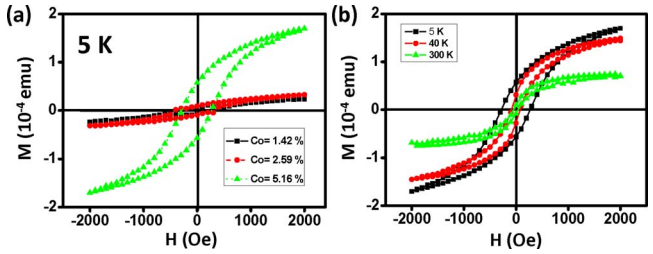

FIG. 3. (Color online) (a) *M-H* curves of $Co_xZn_{1-x}S$ nanowires with different Co contents at 5 K. (b) *M-H* curves of $Co_xZn_{1-x}S$ nanowires with 5.16% Co content at different temperatures.

to several tens of micrometers. A typical x-ray diffraction (XRD) spectrum was used to determine the crystal structure and phase of $Co_xZn_{1-x}S$ nanowires of different doping concentrations [Fig. 1(b)]. In addition to Al_2O_3 {11-20} peak, other peaks are indexed to a wurtzite structure ZnS, and no other phases, such as Zn, Co, and $CoCl_2$, were detected, revealing that all the as-synthesized products are of pure hexagonal wurtzite structure ZnS.

The determinations of the structure and the concentration of Co in ZnS nanowires were carried out using transmission electron microscopy (TEM) (JEOL JEM-2010), which was equipped with an energy dispersive x-ray spectrometer (EDS). Figure 2(a) is a low-magnification TEM image of an individual $Co_xZn_{1-x}S$ nanowire grown with 0.4 g cobalt chloride powders, showing that its surface is clean and diameter is very uniform. The quantitative elemental distributions in cobalt at. % from three different parts of nanowires are also labeled in Fig. 2(a). The results show that the distributions of Co inside nanowires are uniform and the average percentage of nanowires is about 2.59%. We have examined several nanowires of each sample, and the average at. % of 1.42% and 5.16% were detected for 0.2 and 0.6 g of cobalt chloride, respectively. The corresponding selected area electron diffraction (SAED) pattern taken from the $Co_xZn_{1-x}S$ nanowire of Fig. 2(a) is shown in Fig. 2(b), recorded along the [001] zone axis, which reveals the single-crystalline nature of the sample. The SAED can be indexed to a wurtzite structure ZnS, which is consistent with the results obtained from XRD. The TEM image and the corresponding SAED of the $Co_xZn_{1-x}S$ nanowire with 5.16% Co content are shown in Figs. 2(c) and 2(d), respectively. The tails of diffraction spots indicate that the nanowire has planar defects. Figure 2(e) is the atomic resolution TEM image taken from the marked area of Fig. 2(c). It shows that the growth direction of the nanowire is generally along the [0001] orientation, and the arrows in Fig. 2(e) point out the planar defects in the nanowire. The ionic radius of Zn^{2+} and Co^{2+} are 0.074 and 0.0745 nm, respectively. This difference induces the stain when Co ions replace Zn ions at Zn sites. Strain becomes large when Co content increases. In such a case, strain in the nanowire is mostly released by creating planar defects, which implies the Co ion incorporation within the ZnS nanowires by means of systematical substitution for Zn ions. Figure 2(f) is the EDS spectrum revealing that the nanowires are composed of Zn, S, and Co. The Cu peak of the EDS spectrum is contributed from copper mesh. Since a Au thin film was introduced in the synthesis and Au droplets were seen at the top of nanowires in SEM and TEM, the growth mechanism of nanowires can be well understood on the basis of the VLS mechanism.[17]

The magnetic properties of $Co_xZn_{1-x}S$ nanowires were carried out using SQUID magnetometry. Figure 3(a) shows the hysteresis loop of the magnetization M as a function of the applied magnetic field H (M-H curves) of $Co_xZn_{1-x}S$ nanowires with different Co contents at 5 K, showing that these $Co_xZn_{1-x}S$ nanowires are magnetic. The loops of samples with low Co content show weak magnetization, and the saturation magnetization dramatically increases with the Co content in ZnS. The hysteresis loops of nanowires with 5.16% Co at 4, 40, and 300 K are clearly observed in Fig. 3(b). The saturation magnetizations M_s at 4, 40, and 400 K are 1.7×10^{-4}, 1.49×10^{-4}, and 7.45×10^{-5} emu, respectively. Both XRD and TEM results show the absence of the second phase in samples. Therefore, magnetization of $Co_xZn_{1-x}S$ nanowires may arise from the magnetic exchange interaction between Co ions.[18,19]

$Co_xZn_{1-x}S$ nanowire devices were made with the aid of focus ion beam (FIB). Nanowires were first dispersed on Si substrates with a 300 nm SiO_2 top layer, which have Au/Ti prepatterns at the top. Then, Pt:Ga were deposited using the FIB system, which was operated at 30 keV to connect prepatterns and nanowires as electrodes. The deposition is under discreet operation to avoid the doping effect on device channels. *I-V* measurements were carried out using the semiconductor characterization system (Keithley 4200). The typical current-voltage (*I-V*) curves of $Co_xZn_{1-x}S$ nanowires with different Co contents are given in Fig. 4. The data show a linear relationship between current and voltage. Linearly *I-V* curves imply the Ohmic contact between semiconductor and metal. However, it is hard to find metals to form Ohmic contacts with ZnS at room temperature due to the low electron affinity of ZnS.[20] FIB systems are capable of operating at high voltage (30 keV). In this work, Ga ion beams with high intensity can modify the contact area of the nanowire surface during Pt deposition by creating the highly disordered interfacial layer to lower the barrier height,[21] resulting in the Ohmic contacts between $Co_xZn_{1-x}S$ nanowires and Pt. In addition, Fig. 4 also reveals the concentration dependence of conductivity in $Co_xZn_{1-x}S$ nanowires. The average conductivities of $Co_xZn_{1-x}S$ nanowires with 1.42%, 2.59%, and 5.16% Co contents are about 6.5×10^{-2}, 1.4×10^{-1}, and 9.6

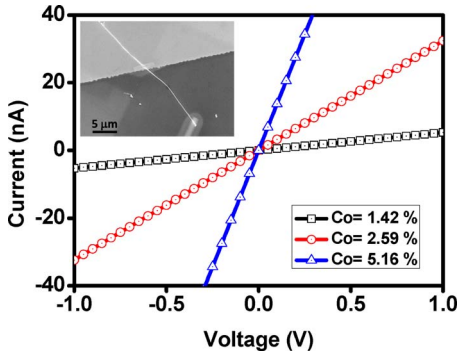

FIG. 4. (Color online) Room temperature *I-V* measurements of $Co_xZn_{1-x}S$ nanowires with different Co contents. The inset shows the SEM image of the nanowire device.

$\times 10^{-1}$ ohm^{-1} cm^{-1}, respectively. The conductivity of nanowires is tuned by introducing different amounts of dopants. The dopants introduced into semiconductors determine their concentrations and affect many of their electrical properties indirectly. The carrier concentrations are mostly affected by dopants. In most cases of semiconductor, the increase in doping concentration leads to the increase in conductivity on the account of excess free carriers.

In summary, DMS $Co_xZn_{1-x}S$ nanowires with different doping levels have been synthesized by the thermal evaporation method. High resolution TEM results showed that $Co_xZn_{1-x}S$ nanowires are wurtzite structured ZnS. Both XRD and EDS analyses demonstrated that Co ions are systematically substituted for Zn ions with homogenous distributions in ZnS nanowires. The magnetic measurements show magnetism of nanowires is still maintained at room temperature. Moreover, the electrical properties of Co-doped ZnS nanowires can be tuned by introducing different doping levels. 3*d*-transition metals have higher solubility (10%–25%) in II-VI compound semiconductors compared to that in III-V compound semiconductors.[22] Thus, these doped nanostructures are expected to open up a number of opportunities for fundamental studies and ensure their potential applications for nanoscale spintronic devices.

This work was supported by DOE BES (Grant No. DE-FG02-07ER46394), NSF (Grant No. DMS 0706436), and National Science Council of the Republic of China (Taiwan) (Grant No. NSC 96-2120-M-007-006).

[1]Y. C. Zhu, Y. Bando, D. F. Xue, and D. Golberg, Adv. Mater. (Weinheim, Ger.) **16**, 831 (2004).
[2]D. Moore, J. R. Morber, R. L. Snyder, and Z. L. Wang, J. Phys. Chem. C **112**, 2895 (2008).
[3]Z. W. Wang, L. L. Daemen, Y. S. Zhao, C. S. Zha, R. T. Downs, X. D. Wang, Z. L. Wang, and R. J. Hemley, Nature Mater. **4**, 922 (2005).
[4]W. Chen, Z. G. Wang, Z. J. Lin, and L. Y. Lin, J. Appl. Phys. **82**, 3111 (1997).
[5]C. Ma, D. Moore, J. Li, and Z. L. Wang, Adv. Mater. (Weinheim, Ger.) **15**, 228 (2003).
[6]M. Y. Lu, P. Y. Su, Y. L. Chueh, L. J. Chen, and L. J. Chou, Appl. Surf. Sci. **244**, 96 (2005).
[7]Y. C. Zhu, Y. Bando, D. F. Xue, and D. Golberg, J. Am. Chem. Soc. **125**, 16196 (2003).
[8]T. Yamamoto, S. Kishimoto, and S. Iida, Physica B **308–310**, 916 (2001).
[9]P. Calandra, M. Goffredi, and V. T. Liveri, Colloids Surf., A **160**, 9 (1999).
[10]M. Bredol and J. Merichi, J. Mater. Sci. **33**, 471 (1998).
[11]Y. Cui, X. Duan, J. Hu, and C. M. Lieber, J. Phys. Chem. B **104**, 5213 (2000).
[12]A. Pan, H. Yang, R. Liu, R. Yu, B. Zou, and Z. L. Wang, J. Am. Chem. Soc. **127**, 15692 (2005).
[13]H. J. Choi, H. K. Seong, J. Chang, K. I. Lee, Y. J. Park, J. J. Kim, S. K. Lee, R. He, T. Kuykendall, and P. Yang, Adv. Mater. (Weinheim, Ger.) **17**, 1351 (2005).
[14]C. Liu, F. Yun, and H. Morkoc, J. Mater. Sci. **16**, 555 (2005).
[15]J. K. Furdyna, J. Appl. Phys. **64**, R29 (1988).
[16]S. J. Pearton, W. H. Heo, M. Ivill, D. P. Norton, and T. Steiner, Semicond. Sci. Technol. **19**, R59 (2004).
[17]R. S. Wagner and W. C. Ellis, Appl. Phys. Lett. **4**, 89 (1964).
[18]T. M. Giebultowicz, P. Klosowski, J. J. Rhyne, T. J. Udovic, J. K. Furdyna, and W. Giriat, Phys. Rev. B **41**, 504 (1990).
[19]C. J. Chen, W. Gao, Z. F. Qin, W. Hu, M. Qu, and W. Giriat, J. Appl. Phys. **70**, 6277 (1991).
[20]M. Aven and C. A. Mead, Appl. Phys. Lett. **7**, 8 (1965).
[21]A. A. Iliadis, S. N. Andronescu, W. Yang, R. D. Vispute, A. Stanishevsky, J. H. Orloff, R. P. Sharma, T. Venkatesan, M. C. Wood, and K. A. Jones, J. Electron. Mater. **28**, 136 (1999).
[22]H. Katayama-Yoshida and K. Sato, J. Phys. Chem. Solids **64**, 1447 (2003).